

Three-Dimensional Laser Velocimeter Investigation of Turbulent, Incompressible Flow in an Axisymmetric Sudden Expansion

G. L. Morrison,* G. B. Tatterson,† and M. W. Long‡
Texas A & M University, College Station, Texas

An experimental study of the flow in an axisymmetric sudden expansion was carried out using a three-color, three-component laser Doppler velocimeter with computer controlled data acquisition and reduction. The area ratio of the expansion was 121:1 and the Reynolds number, which was based on inlet average velocity and inlet diameter, was 22,000. The axial, radial, and circumferential components of the mean velocity were computed from the measurement of three independent velocity components as were the turbulence intensities and kinetic energy. The results showed the flow to be axisymmetric, with negligible circumferential mean velocity. The nature of the separated flow region was consistent with that of previous studies. The large area ratio had little effect on the location of the reattachment, which occurred approximately six step heights downstream of the expansion. All three normalized turbulence intensities were shown to be of the same order of magnitude, thus showing nearly isotropic turbulence. The centerline velocity decay for this large area ratio was much more rapid than the decay for smaller area ratios and was similar to that of a free jet exhausting to atmospheric pressure.

Nomenclature

- AR = area ratio of pipe expansion
- D = jet diameter, inlet pipe diameter
- H = sudden expansion step height
- r = radial distance from centerline
- R_j = initial jet radius, inlet pipe radius
- R_2 = expansion tube radius
- Re_D = Reynolds number (DU_0/ν)
- U_0 = average inlet velocity, jet inlet velocity
- u'_z = rms fluctuating axial velocity component
- u'_2 = rms fluctuating velocity component in a direction of 15 deg from the azimuthal axis
- u'_3 = rms fluctuating velocity component in a direction of -15 deg from the azimuthal axis
- V_r = mean radial velocity
- V_z = mean axial velocity
- V_θ = mean circumferential velocity
- Z = axial distance from expansion
- Z_r = reattachment length
- α = laser beam intersection angle
- ϵ = turbulence dissipation rate
- k = turbulence kinetic energy
- λ = laser light wavelength
- ν = kinematic viscosity

Introduction

SEPARATED flows commonly occur in engineering practice. One particular separated flow is an axisymmetric sudden expansion. This flow is of interest because the region of recirculation, where large pressure losses occur, can be used to advantage as a flame holder for sudden dump combustors. This geometry also occurs frequently in heat exchangers.

Several experimental studies¹⁻³ have shown that, for the abrupt pipe expansion and the similar orifice plate, the levels of the heat/mass transfer coefficient on the downstream side are several times greater than that for fully developed turbulent flow at the same Reynolds number. This is due to the unsteady nature of the flow and surface renewal phenomena that promote transport. Thus, a detailed knowledge of the flowfield can be of great value. Aside from the physical significance arising from this geometry, the data on axisymmetric sudden expansion can be used to verify turbulence models.

Literature Review

Flowfield Studies

In the region of unsteady recirculation, mean velocities are low and the flow is highly turbulent. Because of these flow characteristics, measurements in the recirculation zone have been difficult to obtain with conventional techniques, such as pitot tubes and hot-wire anemometry, due to their inability to measure adequately flow fluctuations in excess of 30% of the local mean velocity. Pitot tubes and hot-wire anemometry also have probe disturbance associated with their use. With the laser Doppler velocimeter (LDV), however, such information about recirculating flows can be obtained.

A complete description of the principles of laser Doppler velocimeters is given in Goldstein.⁴ This technique has many desirable qualities: no physical probe to intrude on the flow, high spatial resolution, linear response, and the capability of determining the direction of the velocity component being measured. The last feature is particularly important in sudden expansion flows where recirculation zones are present or when flows are reversing direction. Reynolds numbers, based on average inlet velocity and inlet diameter, typically range from 10^4 to 10^5 for the sudden expansions previously studied. In the present study, the Reynolds number, based on average inlet velocity and inlet diameter, was 2.22×10^4 . Air, seeded with atomized water, was the working fluid.

Table 1 lists a compilation of recent investigations of axisymmetric sudden expansions and includes those turbulent studies pertinent to this work. All previous studies of axisymmetric sudden expansions have had area ratios ranging from

Received Oct. 10, 1986; revision received Nov. 16, 1987. Copyright © American Institute of Aeronautics and Astronautics, Inc., 1988. All rights reserved.

*Associate Professor of Mechanical Engineering. Senior Member AIAA.

†Associate Professor of Mechanical Engineering.

‡Graduate Student; currently at LTV, Dallas, TX.

Table 1 Details of previous axisymmetric sudden expansion investigations

Author(s)	Techniques	Fluid	Inlet velocity or Reynolds number	Step height Area ratio (H or AR)	Maximum u'_z/U_0 , %	Recirculation zone u'_z/U_0 , %
Macagno and Hung ⁹	Numerical, aluminum powder visualization	Oil	$36 < Re_D < 4500$	$AR = 2.0$	—	—
Back and Roschke ¹⁰	Dye studies	Water	$20 < Re_D < 4200$	$AR = 2.6$	—	—
Freeman ¹²	LDV (one-component)	Water	$Re_D = 3 \times 10^4$	$AR = 2.1$	18	8
Gosman et al. ²⁵	Numerical	Air	$Re_D = 5 \times 10^4$	$AR = 2.6$	6	4
Moon and Rudinger ¹³	Numerical, LDV (one-component)	Air	$1.6 \times 10^5 \leq Re_D \leq 3.7 \times 10^5$	$AR = 1.43$	—	—
Drewry ¹¹	Pressure taps, gas sampling, oil visualization	Air	$8.7 \times 10^5 \leq Re_D \leq 1.9 \times 10^6$	$AR = 1.28$ 1.536 1.92	—	—
Kangovi and Page ⁵	Pressure taps, pitot tubes, hot-wire	Air	$2.4 \times 10^5 \leq Re_D$	$AR = 1.26$ 1.60 1.86 2.27	30	14
Stevenson et al. ¹⁷	Numerical, LDV (one-component)	Air	$Re_D = 4.1 \times 10^4$	$AR = 3.52$	24	2
Stevenson et al. ²⁰	LDV (one-component)	Air	$Re_D = 2.7 \times 10^4$	$AR = 4.00$	21	8
Thompson et al. ⁶	LDV (one-component)	Air	$Re_D = 7.1 \times 10^4$	$AR = 7.29$ 3.61	23	10
Present study	LDV (three-component)	Air	$Re_D = 2.2 \times 10^4$	$AR = 121$	16	4

1.28:1–7.29:1 (see Table 1). This study involves an area ratio of 121:1 where lower recirculation velocities and more rapid centerline velocity decay are expected.

Primary Recirculation Zone

The streamwise distance between the point of separation and reattachment for the primary recirculation zone for axisymmetric sudden expansions has been the subject of many investigations. Back and Roschke¹⁰ performed dye studies to observe the effect of inlet Reynolds number (range of 20–4200) on shear layer growth and reattachment length. The reattachment length initially increased with an increase in Reynolds number and peaked at a value of 25 step heights for a Reynolds number of 290. At this point, not all flow disturbances were damped out and laminar flow instabilities became visible. For the Reynolds number range of 290–1000, the reattachment length rapidly decreased to a minimum value, at $Re = 1000$, of approximately 7 step heights. For the Reynolds number range of 1000–3000, the reattachment length slowly increased to a maximum value of 9 step heights. This value of nine step heights was nearly constant up to $Re = 4200$.

An experimental study was performed by Drewry¹¹ on the axisymmetric sudden expansion in a ramjet combustor using flow visualization and wall static pressure measurements. He found that the reattachment point was between 7.9 and 9.2 step heights for all geometries tested. Freeman¹² measured streamwise velocities of water in the turbulent flowfield of an axisymmetric sudden expansion (oriented vertically, $AR = 2.1$) using a one-component LDV system. Reattachment was found to occur at 8.7 step heights.

Moon and Rudinger¹³ made a series of LDV measurements on an axisymmetric sudden expansion ($AR = 1.43$), using both a one-color, one-component and a two-color, two-component system for Reynolds numbers from 1.6 – 3.7×10^5 . Their data showed that the flow reattachment occurred between 8 and 9 step heights. They also found that the downstream flow of the sudden expansion was axisymmetric.

Kangovi and Page⁵ determined the location of the reattachment point by employing an orifice dam, a fence, and a dual-element pitot probe. The results of these measurements showed the reattachment point to be about 8 step heights downstream of the expansion plane.

DeRossett¹⁶ investigated the turbulent flow over an axisymmetric backstep. The point of reattachment was located 5 step heights downstream and was insensitive to changes in step height and boundary-layer thickness. However, the region over which reattachment occurred was found to broaden with an increase in step height or initial boundary-layer thickness. DeRossett and Przirembel⁷ confirmed this position by using a dual-element hot-film probe to record the temporal variation of the reattachment region associated with an axisymmetric backstep. The large-scale fluctuation frequencies of the flow in the reattachment area were of the order of several hundred cycles per second.

For the area ratios found in the literature (1.28–7.29), reattachment was contained between 6 and 9 step heights for fully turbulent inlet flow conditions. Eaton and Johnston¹⁴ suggested that part of the variation of reattachment length for similar geometries and inlet flow conditions was the result of the recirculation zone slowly shrinking and growing, causing the reattachment point to oscillate. Kuehn⁵ suggested that most of the variation in the reattachment length was attributed to adverse pressure-gradient effects and differences in inlet conditions.

Secondary Recirculation Zone

The difficulty in measuring the mean velocities in the recirculation region is due to the low velocities (typically 1% of the inlet velocity) present in this region. Kangovi and Page⁵ used static pressure taps and hot-wire anemometry to identify the presence of a weak secondary recirculation zone that extended out to one step height from the expansion plane. This secondary region appeared to be the result of the inability

of the primary recirculatory flow to negotiate a 90 deg turn as it approached the backstep from the downstream side. Thompson et al.⁶ showed that this secondary recirculation zone extended from $r/R = 0.7$ out to the wall in the radial direction and from $x/H = 0$ to 1.2 in the axial direction.

DeRossett and Przirembel⁷ observed the secondary separation region immediately downstream of the step face using wall static pressure taps. The region was characterized by a forward flow immediately behind the step followed by a rapid transition to a predominately reversed flow. The water-flow experiments made by Abbott and Kline⁸ documented this type of counter-rotating vortex pattern to be approximately one step height in length over a wide range of step height-to-upstream flow width ratios. DeRossett and Przirembel⁷ found this region to be characterized by a forward flow near the wall extending approximately 1.5 step heights downstream. The counter-rotating flow was independent of changes in the experimental parameters. However, due to the small size of the region and the relatively low velocities, more detailed information was not obtained.

Numerical Studies

Turbulent sudden expansion flows have received varied analytical treatment in recent years. Probably the most popular computer codes for this turbulent flow problem utilize the two-equation $k-\epsilon$ model originally developed by Harlow and Nakayama,²² which has been modified by Launder and Spalding²³ and Launder et al.²⁴ Moon and Rudinger¹³ and Stevenson et al.¹⁷ generated predictions for axisymmetric sudden expansions using the $k-\epsilon$ turbulence model. The two-dimensional, time-averaged transport equations in elliptical form were solved using refined finite-difference techniques.

The $k-\epsilon$ turbulence model requires several constants of proportionality to be used. There are certain values of these coefficients which are generally accepted as universally valid. Moon and Rudinger¹³ showed that these coefficients were not, in fact, universal, at least not for recirculating flows. Stevenson et al.¹⁷ found that although the $k-\epsilon$ model was adequate for engineering purposes, it did not yield a precise representation of the flowfield.

Gosman et al.²⁵ performed a numerical investigation of axisymmetric sudden expansions using the two-dimensional, time-averaged Navier-Stokes equations, and $k-\epsilon$ turbulence modeling. They, like Stevenson et al.¹⁷, found that the models gave inaccurate representations of the flowfield. The dissipation equation was believed to be the major contributing factor in the deficiency.

Objectives of the Present Study

The objectives of the present study were to measure the mean velocity field of a high aspect ratio sudden expansion (including the recirculation regions), to determine the magnitude of the turbulence intensity in three different flow directions, and to provide a data base for a separated flow having a transitional Reynolds number. The data were compared to both free jets and low aspect ratio sudden expansions to observe the effects of the large aspect ratio upon the decay of the mean flow, turbulence intensities, and reattachment length.

Experimental Apparatus

Test Section

The experimental test section is shown in Fig. 1. The flow conditioning system, which supplied air to the test section, consisted of a 15.24-cm i.d. PVC stilling chamber connected to a third-order polynomial contoured nozzle. To eliminate large-scale velocity and pressure nonuniformities, dissipate the turbulence, and straighten the flow, the stilling chamber had perforated plates, screens, and a honeycomb geometry of soda straws. The contraction ratio from the stilling chamber to the nozzle exit was 144:1. A thermocouple and static pressure tap

in the 15.24-cm pipe was used to obtain the stagnation temperature and pressure, respectively.

Immediately following the nozzle was an expansion ring assembly, containing 7.62 cm of 12.7 mm i.d. cast acrylic tubing that matched the nozzle exit diameter. The 12.7-mm tube exited from the expansion ring assembly into a 13.97-cm i.d. glass tube. This glass tube did not contain visible striations and was 1.22 m in length. A 1.83-m acrylic tube with the same diameter as the glass tube was attached downstream of the glass tube to help minimize exit effects in the glass tube. In order to keep the air at a nearly constant temperature (20 °C), an air-water heat exchanger was employed. After passing through water separator/filters, the flow rate was controlled by a pressure regulator and a fine threaded flow control valve.

Laser Doppler Velocimeter System

Flowfield measurements were made using a three-color, three-component laser Doppler velocimeter system consisting of three dual-beam subsystems. The optical components were supplied by TSI Inc. Argon-ion laser wavelengths of 514.5 nm (green), 488 nm (blue), and 476.5 nm (violet) were used where each color facilitated the measurement of one noncolinear component of the velocity vector (see Fig. 2). The optical train for each color employed light polarization units, acousto-optical modulators, and beam expanders. The acousto-optical modulators introduced a 40 MHz frequency shift in one of the beam pairs for all three colors. This frequency shift effectively eliminated all fringe bias since the shift frequency was large compared to the Doppler frequency. The light reflected from the seed particles was collected in an off-axis, backscatter mode at an angle of 30 deg from the axis of the optical train transmitting the light. There were two optical trains whose axes intersected at a 30 deg angle, with one optical train mounted above the other. These two optical trains are shown in Fig. 2. The lower train transmitted the blue and green light and collected light scattered from the violet beam intersection, while the top train transmitted the violet light and collected light scattered from the green and blue beams intersections. The composite measurement volume produced by the intersection of all six beams was $0.025 \times 0.025 \times 0.102$ mm. Three photomultiplier tubes (PMT's), each sensitive to only a specified color, were used to measure the scattered light. The entire

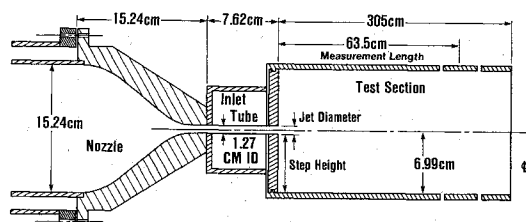


Fig. 1 Test section.

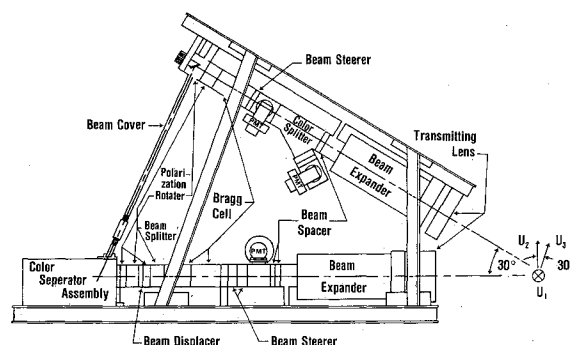


Fig. 2 Laser velocimeter system.

Table 2 LDV system parameter settings

Optical system settings	Green	Blue	Violet
$\lambda_0, \lambda_1, \lambda_2$ (laser light wavelength)	514.5 nm	488 nm	476.5 nm
$\alpha_0, \alpha_1, \alpha_2$ (beam intersection angle):	14.72 deg	15.56 deg	14.60 deg
F_R (fringe spacing):	2.01 μm	1.80 μm	1.87 μm
Probe volume size (waist diameter):	0.0246 mm	0.0233 mm	0.0228 mm
F_s (frequency shift): 40 MHz			
Data collection settings			
Mode of operation: Total burst count			
Electronic filter settings: 100 MHz low pass 20 MHz high pass			
Number of fringes/signal (N): 8			
Comparator: 1 (1%)			
Sample size: 1000/channel			
Data rate: > 100,000 samples/s/channel			
Sample rate: 50–100 samples/s/channel			
Flow system parameters			
U_1 (inlet average velocity): 25.5 m/s \pm 0.5 m/s			
Re_D (based on inlet velocity): 2.22×10^4			
H (step height): 2.5 in.			
R_j (inlet radius): 0.25 in.			
R_2 (outlet radius): 2.75 in.			
Seed particles: H_2O			
Seed particle size: 1 μ			

optical system (laser and optics) was mounted on a three degree-of-freedom traversing system which located the measurement volume position in space with a resolution of 0.0025 mm (repeatable to 0.01 mm). Table 2 presents the operating conditions of the laser and test section for this study.

The seeding system consisted of two in-line six-jet atomizers (TSI 9306), using water as the seeding material. This system produced spherical seed particles approximately 1 μm diam, which ensured that they followed the flow with peak visibility of the Doppler signal.²⁶

For this particular study, coincidence measurements were not made. The lens effect of the cylindrical tube caused the crossings of the three sets of beams to move at different rates as the beams were traversed in the radial direction. The refraction of the light beams as they passed through the cylindrical wall was determined for the calculation of the sampling volume's spatial location.

Measurements were performed from $r/R_2 = 0$ to 0.984 (1.125 mm from the expansion pipe's inner wall) and for an axial distance of 10 step heights ($0 \leq z/H \leq 10$). In the region of the flow reattachment, axial traverses were performed at $r/R_2 = 0.991$ (6.25 mm from the expansion pipe's inner wall). Full-length axial traverses ($0 \leq x/H \leq 10$) were made every $0.05R_j$ from $0 \leq r/R_j \leq 4$ ($0 \leq r/H \leq 0.4$) then every $0.10R_j$ to the expansion pipe wall. The axial measurement locations were spaced $0.25R_j$ from the expansion plane to $z/R_j = 16$ ($z/H = 1.6$), then spaced $2R_j$ to $z/R_j = 56$, and then $4R_j$ from 56 to $100 z/R_j$.

Data Acquisition

The outputs of the photomultiplier tubes were analyzed by three counter systems (TSI 1990B). Each counter compared the frequency determined from five cycles of the Doppler burst to the frequency determined from eight cycles. If these two measured frequencies differed by more than 1%, the data were discarded. The entire system was interfaced to a PDP 11/23 + computer system that controlled the traverse table, recorded the instantaneous data supplied by the signal processors, converted this data into an instantaneous velocity vector, and stored the results. Since the laser optics were set to measure three non-colinear velocity components, the three orthogonal mean velocities were calculated from the three non-colinear mean velocities measured directly. The computer

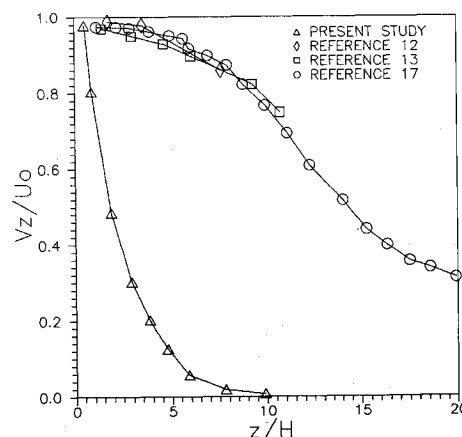


Fig. 3 Mean centerline velocity distribution.

system also analyzed all of the instantaneous data acquired at a spatial location by computing the mean velocity, turbulence intensity, and other statistics.

Results and Discussion

Mapping of the axisymmetric sudden expansion flowfield required both direct velocity measurements, indirect computations of the three orthogonal mean velocity components, and the determination of various turbulent parameters. The flow and turbulent parameters obtained were:

- 1) Mean velocities V_z , V_θ , and V_r ,
- 2) turbulence parameters u'_z , u'_θ , u'_r , and $3u'^2_z/2U_0^2$ which approximates the turbulence kinetic energy, and
- 3) Reattachment length.

Centerline Mean Velocity and Turbulence Intensity Distributions

Similarity existed between the centerline parameters for the flow just downstream of the step for a turbulent sudden expansion and the near-field region of a free jet, since both flows had a core region in which the centerline velocity was maintained and was followed by a region of centerline velocity decay. From the previous studies^{6,12,13,17} of sudden expansions, the decay was nearly independent of step height (for

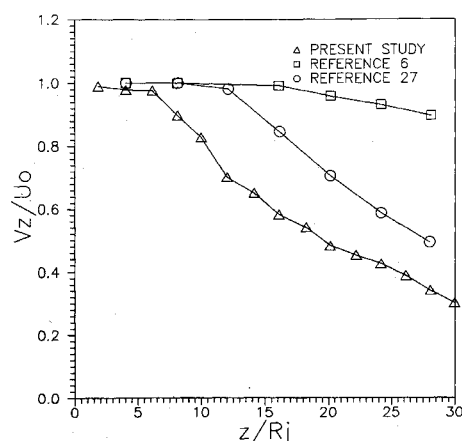


Fig. 4 Mean centerline velocity distribution.

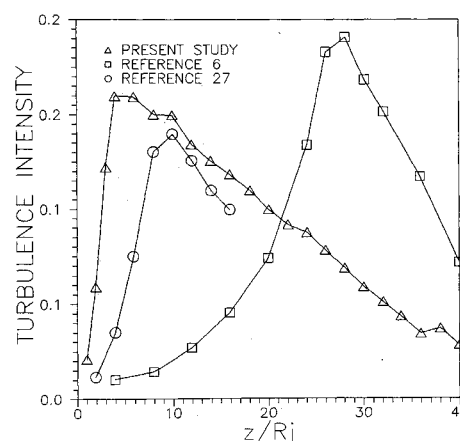


Fig. 5 Centerline turbulence intensity distribution.

$AR = 1.3$ to 7.3). Figure 3 shows the mean centerline velocity decay in this study along with the corresponding sudden expansion data from Freeman,¹² Moon and Rudinger,¹³ and Stevenson et al.¹⁷ The data obtained in the present study showed a large deviation from previous studies with lower area ratios.^{12,13,17} This large area ratio effect appears in other figures in this work as well.

Figure 4 shows mean centerline velocity distributions that have been nondimensionalized by the inlet jet radius for the free jet data from Crow and Champagne,²⁷ the sudden expansion data from Thompson et al.⁶ ($AR = 3.61$), and the present study. The effects of area ratio and Reynolds number on the rate of velocity decay are shown. The free jet data from Crow and Champagne²⁷ were for an inlet Reynolds number based on the diameter of the jet of 62,000 compared to 22,000 for the present study. The differences between the studies were attributed to differences in potential core lengths. In addition, the straight pipe (length of six inlet diameters) at the nozzle exit for the present study enabled a boundary layer to develop that was thicker at the pipe exit than the boundary layer of Crow and Champagne²⁷ where the flow exited a short nozzle.

The slope of the mean velocity decay past the potential core in the present study was very close to that of the free jet. This was expected since enlarging the area ratio to 121 was effectively approaching a free jet geometry.

Figure 5 shows the axial centerline turbulence intensity, normalized with the average inlet velocity, along with the corresponding data from Thompson et al.⁶ and Crow and Champagne.²⁷ The jet data were only available to $z/R_j = 16$. As expected, the turbulence intensity in the core immediately downstream of the expansion ($z/R_j = 1.0$) was quite low (2%) but rose quickly to a maximum of 16% at $z/R_j = 4$ for the present study. Within the first step height, the centerline turbulence intensity reached maximum level. The other sudden expansion study⁶ showed a peak at approximately $z/R_j = 28$ while the free jet²⁷ peaked at $z/R_j = 8$.

The occurrence of the earlier peak in the axial centerline turbulence intensity of the present study was due to a more rapid centerline velocity decay because of the large area ratio. This occurred earlier than that of the free jet study of Crow and Champagne²⁷ due to the lower inlet Reynolds number and thicker initial boundary layer of this study. Both the free jet and the present study's turbulence intensity decay were quite similar past their respective peaks and the rates of decay were very similar to $z/R_j = 16$.

Mean Velocity Distributions

The mean velocity component distributions were obtained from direct LDV measurements. Figures 6a and 6b show the measured mean axial and radial velocity contours, normalized

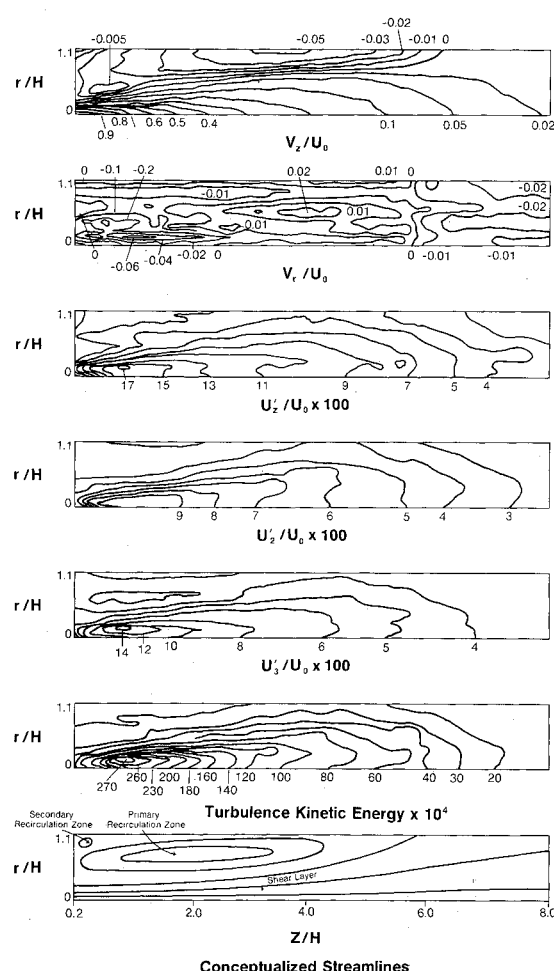


Fig. 6 Flowfield contours.

with U_0 . The mean azimuthal velocity distributions are not presented here since these were zero throughout the flowfield.

Axial Velocity

The axial velocity remained constant on the centerline of the flow for the first 0.6 step heights indicating the presence of a potential core region. The width of the core region continually diminished in the axial direction and disappeared before the first step height. Thompson et al.⁶ observed that, for a sudden expansion area ratio of 3.61, the velocity profiles were

flat across the potential core region, up to 6 step heights downstream from the expansion, and that the width of the core region had disappeared at 8 step heights downstream from the expansion.

The mean axial velocity decayed rather quickly in the four step heights downstream from the expansion. The magnitudes of the mean velocity were only slightly changed in the region from 8 to 10 step heights and are not presented here. The redeveloped flow, ($Z/H > 8$, where the flow began to look like fully developed pipe flow) with a Reynolds number of less than 200, was relaminarizing. The flow exiting from the extension duct (48 step heights) was observed to be laminar, by heavily seeding the flow so that the flow was visible. Eaton and Johnston⁴ predicted that for fully turbulent redeveloping flow, complete redevelopment of turbulent pipe flow did not occur until at least 50 step heights downstream of the expansion.

Recirculation Zones

Figure 6a shows the location of the zero axial velocity contour line and the nature and magnitude of the primary recirculation zone, which is depicted conceptually in Fig. 6g. The maximum axial recirculation velocity (negative value) was approximately 5% of the inlet centerline velocity and was located from about 3–4 step heights downstream from the expansion. All of the previous studies of axisymmetric sudden expansions showed the maximum recirculation velocities were between 10 and 20% of the inlet centerline velocity. The lower value in the present study can be predicted, however, by applying mass conservation to the differing geometries. In Fig. 6a, the flow reattaches just after the sixth step height as designated by the zero velocity contour line intersecting the wall. Measurements were made in much greater detail in the reattachment area and the results will be presented later.

A secondary recirculation zone can also be identified in Fig. 6a and is also depicted in Fig. 6g. This zone was driven by the backflow of the primary recirculation zone approaching the step from the downstream side. The exact location and nature of the zone is not well defined in this figure, but appears to extend to $z/H = 0.8$ and is designated by positive values of the axial velocity in the corner of the expansion. This value for the "secondary reattachment" point was in good agreement with the wall shear stress measurements of Kangovi and Page⁵ and the LDV measurements of Thompson et al.⁶ Both investigations showed that this region extended approximately one step height downstream. The magnitude of the maximum secondary zone forward flow in the present study was 1.5% of U_0 , which also agreed with the value obtained by Thompson et al.⁶

Radial Velocity

Figure 6b shows the radial mean velocity contours. The maximum negative radial mean velocity occurred at $r/H = 0.22$ and in the region from about 1–2 step heights in the axial direction. This was due to the entrainment of the relatively still fluid into the expanding shear layer. Figure 6b shows that near the wall, from the expansion to $z/H = 5.5$, all radial components of the mean velocity are positive, that is, flowing toward the wall. The maximum radial velocity in this region was about 1.6% of U_0 and was assumed to be caused by interaction with the wall boundary layer.

Turbulence Intensities

Figures 6c–e show the three normalized turbulence intensities given in percent. The fluctuating component u'_z was in the axial direction, and u'_2 , u'_3 were ± 15 deg from the azimuthal axis; all were nondimensionalized with the pipe exit velocity U_0 . As expected, fairly low levels of turbulence were present in the central core of the inlet flow, whereas large levels of turbulence were present in the shear layer at the edge of the inlet pipe. The data showed that the axial turbulence intensity

normalized by the average inlet velocity varied from 2.2% in the core region to 19.6% in the shear layer, the second component from 1.6 to 12%, and the third component from 1% in the core region to 17% in the shear layer. The peak turbulence intensities also identified regions of high shear and mixing. By comparison, maximum values of normalized turbulence intensity measured for backward facing step flows were 21% by Eaton and Johnston⁴ and 19% by Bremmer et al.¹⁹

The maximum turbulence intensity and the turbulence intensity in the recirculation zone for sudden pipe expansions are listed in Table 1. The measured values of maximum turbulence intensity range from 18–30%, which agreed with the values measured in the present study, which averaged 16%. Gosman et al.²⁵ numerically predicted the turbulence kinetic energy of the flow. If isotropic turbulence was assumed, then an estimated value of 6% would be obtained for maximum turbulence intensity. However, this is substantially lower than any of the measured values in the figure. Figures 6c–e show that the peaks in the normalized turbulence intensity for all three components occur at the same spatial location ($z/H = 0.8$, $r/H = 0.15$) and broaden as the shear layer spread in the downstream direction. As the shear layer spread, a decrease in the maximum turbulence intensity occurred.

The general form of the peaks in the axial turbulence intensity was in agreement with that presented by Stevenson et al.¹⁷ With the much faster centerline velocity decay of the large area ratio geometry used in the present study, the shear layer spread more rapidly and the turbulence intensity peaked and decayed much faster.

The form of the axial turbulence intensity contours as their magnitude decreased in the recirculation region of the present study was in agreement with the studies of Stevenson et al.,¹⁷ Thompson et al.,⁶ and Freeman.¹² However, differences were also evident. Most of these past investigations showed the axial turbulence intensity to level off near the wall to a value of about 8%, whereas the present study showed a near-constant level of 4% within one inlet diameter of the wall. As expected, the magnitudes of the turbulence intensities in the entire recirculation region were greater in the previous investigations. This was due to the greater dissipation of turbulence into the larger quiescence volume in the present study. However, the predictions of the turbulence kinetic energy by Gosman et al.,²⁵ when used to estimate the turbulence intensity, predicted a 4% turbulence intensity.

The maximum values of axial turbulence intensity obtained in the mixing layer region of the flowfield were compared to those in a round free jet as reported in Hinze.²⁸ In a free jet, the profiles at each axial location were self similar if the velocities were normalized with the centerline mean velocity at that location. The axial turbulence intensities, measured in the mixing layer, were normalized with the local centerline velocity in the present study and were found to increase from 23% at $z/H = 1$, to 45% at $z/H = 0.4$. In comparison, the free jet data from Hinze²⁸ showed a peak axial turbulence intensity normalized in this fashion of approximately 28%.

The second and third component turbulence intensities also showed a peak in the shear layer, approaching a constant value in the recirculation region. Generally, all three turbulence intensities were of the same order of magnitude throughout the flowfield, and in the recirculation region had magnitudes in the range of 2–7%. As a result, the recirculation region was one of relatively low isotropic turbulence (based upon the exit velocity).

Downstream of reattachment, the flow redeveloped and became a transitional flow undergoing relaminarization. The three turbulence intensity profilers flattened out with normalized values from 1.5–3.5%. In comparison, the studies of Stevenson et al.¹⁷ and Thompson et al.⁶ showed the fully turbulent redeveloping flow to have nearly isotropic turbulence values of 10–15%. Again, the low level of turbulence in the present study was expected due to the fully developed extension duct Reynolds number of 200.

Figure 6f shows the approximate turbulence kinetic energy profiles normalized by the square of the average inlet velocity. The contours up to $z/H = 6$ show a peak in the kinetic energy distribution which broadens as the mixing zone spreads in the downstream direction. Peaks in the turbulence kinetic energy profiles also identify regions of highest shear and mixing. The maximum turbulence kinetic energy of magnitude 2.3% occurred at an axial distance of approximately one step height and was in the shear layer. The location of this peak coincided with the peaks of the three turbulence intensities. From there, the levels of the turbulence kinetic energy decreased to a uniform level of 0.11%. This low level indicated that the flow was becoming laminar-like.

Local Turbulence Levels and Induced Errors

The recirculation zones and the far downstream locations showed turbulence levels of less than 4% based upon the exit velocity in this study. However, when nondimensionalized by the local velocity, these values exceed 1000% of the mean local velocities. This level of fluctuation was also observed by Stevenson et al.²⁰ in the recirculation zone. Since the laser velocimeter was measuring discrete samples of the velocity generated by the occurrence of a speed particle in the measurement volume, the capability of the anemometer to follow the fluctuations was not a major concern.

The statistical biasing of the data due to the large variance of the data was of concern.^{17,18,20,21,29,30} Velocity bias control was attempted by heavily seeding the flow while controlling the processor sampling rate and using the total burst count/velocity bias mode of the signal processor. However, velocity bias and statistical error were still present in the highly turbulent portion of the shear layer as well as in regions of very low mean velocity (hence, very large local turbulence intensity). Increasing the number of samples taken at a point in the shear layer was effective in decreasing the velocity bias.

Errors in the measured values of mean velocity and turbulence intensity were considered to be produced primarily by the accuracy of the counters and velocity bias. The error produced by the counters was quantified by knowing the resolution of the counters and the frequency of the Doppler bursts. In this case, the counters had a resolution of 1 ns, the Doppler burst frequency was centered around the Bragg cell shift frequency of 40 MHz, and the counters measured the time for eight cycles. This resulted in a resolution of the mean velocity of approximately 0.25%.

The statistical error and velocity bias error were more difficult to evaluate. Yanta³⁰ provided a discussion of the statistical error prediction for the mean velocity and standard deviation (turbulence intensity) computed from an ensemble of laser Doppler anemometry data. Yanta³⁰ pointed out that the main factor influencing statistical and velocity bias error was the local turbulence intensity level. The higher the turbulence level, the more uncertainty is present in the flow. Based upon Yanta's calculations, the high levels of turbulence in the recirculation zone and far downstream resulted in a 95% confidence interval of approximately 6% of the mean velocity.

The effect of velocity bias had not been quantified for local turbulence intensities over 30%. At 30%, the error in the mean velocity was about 2%, but it was noted by Yanta³⁰ that as intensity levels increased over 30%, the level of error increased. Based upon our analysis of velocity histograms taken in the present flow for various numbers of velocity realizations under various operating conditions, we estimated an error of about 4% in the shear layer region.

Reattachment Location

It was possible to observe visually the reattachment point after the sixth step height by heavily seeding the flow. Under these conditions, it was seen that the area around the sixth step height was unstable, having large-scale fluctuations with the reattachment point moving up and down the pipe. In order to quantify the average location of the mean reattach-

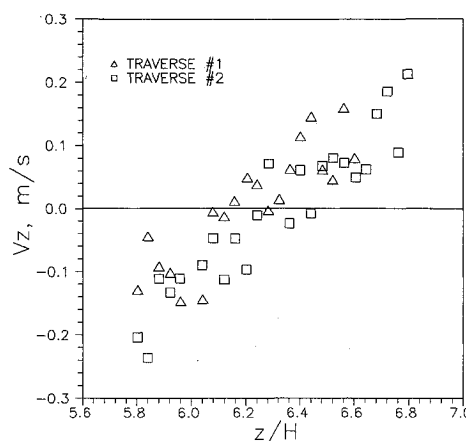


Fig. 7 Axial mean velocity distribution near the reattachment point.

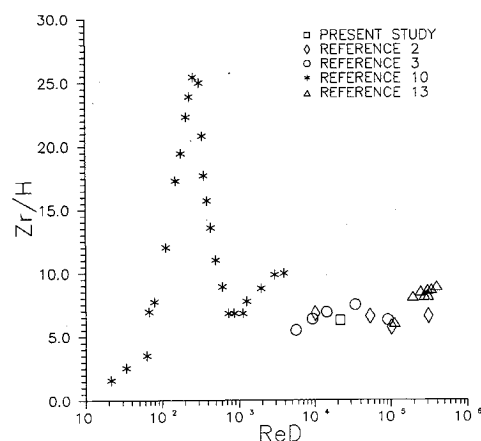


Fig. 8 Reynolds number dependence of the reattachment length.

ment point, two axial velocity traverses were performed near the surface of the pipe wall ($r/R_2 = 0.991$) with the results shown in Fig. 7. From this figure, the flow is seen to change from a reverse to a forward direction. From $z/H = 5.80$ to 6.16, a backflow was present, and from $z/H = 6.40$ to 6.80, the flow was forward. In the region from 6.20–6.36 step heights, both positive and negative values of the axial component were present at each location. The average of the two trials at each point in this region was very close to zero and the zone of reattachment was between 6.20 and 6.36 step heights.

There was close agreement in comparing the location of the reattachment zone in the present study to the results of previous studies (Fig. 8). Most authors found reattachment to be between 6 and 9 step heights. DeRossett¹⁶ and DeRossett and Przirembel,⁷ however, found the zone of reattachment to be at approximately 5 step heights. The spread in the data was believed to be caused by the unsteadiness of the flow in this region of reattachment, as described by DeRossett and Przirembel.⁷

Conclusions

The laser velocimeter was shown to be an effective tool in measuring the velocity and turbulence quantities present in this type of investigation. Of particular use was its ability to measure reverse flow, even at very low velocities.

The centerline velocity and turbulence parameters were nearly identical to those of a free jet, up to 3 step heights downstream of the expansion. A secondary recirculation zone

was identified and found to be quite complex. In order to define fully the flow in this region, a tighter measurement grid and larger measurement groups are needed.

The oscillating reattachment zone was identified and reattachment of the sudden expansion flow did not occur at a single point, but over a range of about 0.2 step heights. In comparing the present area ratio of 121 to the previous studies involving area ratios from 1.3–7.3, there was very little effect of area ratio on the location of reattachment and, as a result, the location of reattachment was not a function of area ratio.

References

- ¹Zemanick, P.P. and Dougall, R.S., "Local Heat Transfer Downstream of an Abrupt Circular Channel Expansion," *ASME Journal of Heat Transfer*, Vol. 92, Feb. 1970, pp. 53–60.
- ²Krall, K.M. and Sparrow, E.M., "Turbulent Heat Transfer in the Separated, Reattached, and Redevelopment Regions of a Circular Tube," *ASME Journal of Heat Transfer*, Vol. 88, 1966, pp. 131–136.
- ³Runchal, A.K., "Mass Transfer Investigations in Turbulent Flow Downstream of a Sudden Enlargement of a Circular Pipe for Very High Schmidt Numbers," *International Journal of Heat and Mass Transfer*, Vol. 14, June 1971, pp. 781–792.
- ⁴Goldstein, R.J. (ed.), *Fluid Mechanics Measurements*, Hemisphere, New York, 1983, pp. 155–244.
- ⁵Kangovi, S. and Page, R.H., "Subsonic Turbulent Flow Past a Downstream Facing Annular Step," *ASME Journal of Fluids Engineering*, Vol. 101, June 1979, pp. 230–236.
- ⁶Thompson, H.D., Stevenson, W.H., and Durrett, R.P., "Laser Velocimeter Measurements and Analysis in Turbulent Flows with Combustion, Part 3," AFWAL-TR-82-2076-PT-3, AD-A146206/8, July 1984.
- ⁷DeRossett, T.A. and Przirembel, C.E.G., "Time-Dependent Behavior of Separated Flow Regions," Instrument Society of America Aerospace Instrumentation Symposium 74255, pp. 273–280, 1974.
- ⁸Abbott, D. and Kline, S.J., "Experimental Investigation of Subsonic Turbulent Flow Over Single and Double Backward Facing Steps," *Journal of Basic Engineering, Transactions of the American Society of Mechanical Engineers, Series D*, Vol. 84, No. 3, Sept. 1962, pp. 317–325.
- ⁹Macagno, E.O. and Hung, T.K., "Computational and Experimental Study of a Captive Annular Eddy," *Journal of Fluid Mechanics*, Vol. 28, Pt. 1, April 12, 1967, pp. 43–63.
- ¹⁰Back, L.H. and Roschke, E.J., "Shear-Layer Flow Regimes and Wave Instability and Reattachment Lengths Downstream of an Abrupt Circular Channel Expansion," *ASME Journal of Applied Mechanics*, Vol. 39, Sept. 1972, pp. 677–681.
- ¹¹Drewry, J.E., "Fluid Dynamic Characterization of Sudden Expansion Ramjet Combustor Flowfields," *AIAA Journal*, Vol. 16, April 1978, pp. 313–319.
- ¹²Freeman, A.R., "Laser Anemometer Measurements in the Recirculation Region Downstream of a Sudden Pipe Expansion," *The Accuracy of Flow Measurements by Laser Doppler Methods*, Proceedings of the LDA Symposium, 1975, pp. 704–709.
- ¹³Moon, L.F. and Rudinger, G., "Velocity Distribution in an Abruptly Expanding Circular Duct," *ASME Journal of Fluids Engineering*, Vol. 99, March 1977, pp. 226–230.
- ¹⁴Eaton, J.K. and Johnston, J.P., "Turbulent Flow Reattachment," Mechanical Engineering Department, Stanford Univ., Stanford, CA, Rept. MD-39, 1980.
- ¹⁵F. Kuehn, D.M., "Effects of Adverse Pressure Gradient on the Incompressible Reattaching Flow over a Rearward-Facing Step," *AIAA Journal*, Vol. 18, March 1980, pp. 343–344.
- ¹⁶DeRossett, T.A., "An Experimental Investigation of Subsonic Steady and Oscillating Flow over an Axisymmetric Back Step," Ph.D. Thesis, Mechanical, Industrial, and Aerospace Engineering Department, Rutgers Univ., New Brunswick, NJ, May 1973.
- ¹⁷Stevenson, W.H., Thompson, H.D., and Luchik, T.S., "Laser Velocimeter Measurements and Analysis in Turbulent Flows with Combustion, Part 1," AFWAL-TR-82-2076-PT-1, AD-A121179/6, Sept. 1982.
- ¹⁸Starner, S.H. and Bilger, R.W., "LDA Measurements in a Turbulent Diffusion Flame with Axial Pressure Gradient," *Combustion Science and Technology*, Vol. 21, March 1980, pp. 259–276.
- ¹⁹Bremmer, R., Thompson, H.D., and Stevenson, W.H., "An Experimental and Numerical Comparison of Turbulent Flow over a Step," AFWAL-TR-80-2105, Dec. 1980.
- ²⁰Stevenson, W.H., Thompson, H.D., and Gould, R.D., "Laser Velocimeter Measurements and Analysis in Turbulent Flows with Combustion," AFWAL-TR-82-2076-PT-2, AD-A131882/3, July 1983.
- ²¹Stevenson, W.H., Thompson, H.D., and Roesler, T.C., "Direct Measurement of Laser Velocimeter Bias Errors in a Turbulent Flow," *AIAA Journal*, Vol. 20, Dec. 1982, pp. 1720–1723.
- ²²Harlow, F.H. and Nakayama, P., "Transport of Turbulence Decay Rate," Los Alamos Science Lab., University of California Report LA-3854, 1968.
- ²³Lauder, B.E. and Spalding, D.B., "The Numerical Computation of Turbulent Flows," *Computer Methods in Applied Mechanics and Engineering*, Vol. 3, March 1974, pp. 269–289.
- ²⁴Lauder, B.E., Morse, A., Rodi, W., and Spalding, D.B., "The Prediction of Free Shear Flows—A Comparison of Six Turbulence Models," *Proceedings of NASA Conference on Free Shear Flows*, Hampton, VA, 1972.
- ²⁵Gosman, A.D., Khalil, E.E., and Whitelaw, J.H., "The Calculation of Two-Dimensional Turbulent Recirculating Flows," *Turbulent Shear Flows I*, Springer-Verlag, New York, 1977, pp. 237–255.
- ²⁶Thompson, H.D. and Flack, R., Jr., "An Application of Laser Velocimetry to the Interpretation of Turbulent Structure," *Proceedings of the ISL/AGARD Workshop of Laser Anemometry*, H. Pfeifer and J. Haertig (eds.), German-French Research Institute, St.-Louis, France, 1976.
- ²⁷Crow, S.C. and Champagne, F.H., "Orderly Structure in Jet Turbulence," *Journal of Fluid Mechanics*, Vol. 48, Aug. 1971, pp. 547–591.
- ²⁸Hinze, J.O., *Turbulence*, McGraw-Hill, New York, 1975, Chap. 6.
- ²⁹Erdmann, J.C. and Tropea, C.D., "Statistical Bias of the Velocity Distribution Function in Laser Anemometry," *Proceedings Application of Laser Doppler Velocity to Fluid Mechanics*, Lisbon, Portugal 1982.
- ³⁰Yanta, W.J., "The Use of the Laser Doppler Velocimeter in Aerodynamic Facilities," AIAA Paper 80-0435, Jan. 1980.